N89-22910

MAGNETIC BEARING STIFFNESS CONTROL USING FREQUENCY BAND FILTERING

H. Ming Chen
Mechanical Technology Incorporated
968 Albany-Shaker Road
Latham, New York 12110, U.S.A.

Active magnetic bearings can be implemented with frequency band-reject filtering that decreases the bearing stiffness and damping at a small bandwidth around a chosen frequency. The control scheme has been used for reducing a rotor dynamic force, such as an imbalance force, transmitted to the bearing stator. This study reveals that the scheme creates additional system vibration modes at the same frequency. It also shows that the amount of force reduction is limited by the stability requirement of these modes.

INTRODUCTION

The attractive-type active magnetic bearings (AMBs) usually have four quadrants of electromagnets (ref. 1). A pair of opposite quadrants independently control the journal motion in one direction by a Proportional-Integral-Derivative (PID) controller (ref. 2). Steady-state (bias) currents are induced in the quadrants so that the total control current in each quadrant never changes polarity. This provides a base for linear feedback control and greatly simplifies the control circuitry (ref. 3).

There appears to be a growing interest in applying the AMBs not only for their advantageous basic bearing function, but also for their potential to be the rotor force isolator (ref. 4). An AMB can be made extra "soft" at narrow frequency bands, and the rotor forces to ground at these frequencies can be dramatically reduced at the sacrifice of large rotor runouts. For example, the well-publicized AMB control feature, "auto-balancing," was designed to reduce imbalance force to ground with the rotor rotating about its inertia axis (ref. 2). However, the creation of these stiffness "valleys" also creates instability problems for the rotor-AMB system. Herein this type of instability problem is addressed analytically while an experimental project is in progress.

NOMENCLATURE

AMB	active magnetic bearing
a	phase-lead network zero parameter
B	frequency bandwidth of band-pass filter
b	phase-lead network pole parameter
C	radial air gap
C_d	proportional feedback gain

C_v	phase-lead feedback gain
C_e	integral feedback gain
C_p	band-pass filter gain
C_{po}	band-pass filter stability threshold gain
F	regulating magnetic force
F_1, F_3	magnetic force per pole due to bias current in quadrant 1 or 3
FODE	first-order differential equation
f	band-pass factor
G	power amplifier gain
I_1, I_3	bias current in quadrant 1 or 3
i	regulating current
j	$\sqrt{-1}$
K	AMB stiffness
K_i	current stiffness
K_m	magnetic (negative) stiffness
LHS	left hand side
M	mass supported by AMB
PID	proportional-integral-derivative
Q	integrator output
R	nondimensional frequency parameter defined at a stiffness valley
RHS	right hand side
S	Laplace variable
t	time
U	real stiffness at ω_c after filter implementation
u	real stiffness at ω_c before filter implementation
u_r	RHS stiffness
u_ℓ	LHS stiffness
V	imaginary stiffness at ω_c after filter implementation
v	imaginary stiffness at ω_c before filter implementation
Y	AMB journal displacement in Y-direction
Y_p	band-pass filter output
Z	phase-lead network output
ΔC_d	net proportional feedback gain contributing to real stiffness
ω	exciting frequency
ω_c	band-pass filter center frequency
ω_ℓ	LHS slope frequency
ω_o	integrator cut-off frequency

ω_r	RHS slope frequency
dot	d/dt
$\Delta\omega$	$\omega_c-\omega$
θ	magnetic pole angle

AMB CONTROL WITH FREQUENCY BAND FILTERING

Assuming the bias currents are much larger than the regulating currents and the air gap is much larger than the journal's normal excursion, the two perpendicular axes of a radial AMB can be controlled independently (ref. 3). A control scheme for each axis is presented in figure 1. There are four parallel loops processing a journal displacement measurement. The top three loops, including a phase-lead network ($b > a$), form a conventional PID controller. The fourth loop comprises a typical second-order band-pass filter with the center frequency at ω_c, bandwidth B, and gain C_p (ref. 5). The filter can have a fixed center frequency or it may vary the center frequency with rotor speed. The latter is called a tracking filter and its implementation was explained by SKF (ref. 6). The filter output is subtracted from the displacement measurement that is fed into the phase-lead network. Also, the output multiplied by a gain ΔC_d is added to the basic PID signals that control the power amplifier. The gain ΔC_d is defined below.

$$\Delta C_d = C_d - K_m/(K_i G) \tag{1}$$

where

C_d = proportional loop gain, volt/m

G = amplifier gain, A/volt

K_m = magnetic stiffness
$= 2\,(F_1/C + F_3/C)\cos\theta$, lb/m

K_i = current stiffness
$= 2\,(F_1/I_1 + F_3/I_3)$, lb/amp

C = radial air gap, m

I_1, I_3 = bias current of quadrants 1 or 3, respectively, A

F_1, F_3 = magnetic forces per pole due to bias currents, N

The parameter K_m is the "negative spring" effect of the AMB magnetic field. The part of the proportional gain to overcome this effect is $K_m/(K_i G)$. Therefore, ΔC_d is the net proportional gain contributing to the AMB stiffness.

Assuming the power amplifiers are current sources in the bandwidth of interest (G = constant), the AMB regulating force across the quadrants 1 and 3 is

$$F = K_i\, i + K_m\, Y \tag{2}$$

From figure 1, the regulating current is

$$i = G\,[\,-C_d\, Y - C_v\, Z - C_e\, Q + \Delta C_d\, C_p\, Y_p] \tag{3}$$

where

$$Z = [(S + a)/(S + b)]\ (Y - C_pY_p) \tag{4}$$

$$Q = [1/(S + \omega_o)]\ Y \tag{5}$$

$$Y_p = [BS/(S^2 + BS + \omega_c{}^2)]\ Y \tag{6}$$

Incorporating equations (4), (5), and (6) into equation (3), which in turn is incorporated into equation (2), the AMB reaction transfer function can be expressed by equation (7).

$$-F/Y = K_iG[(\Delta C_d + C_v(S + a)/(S + b))f + C_e/(S + \omega_o)] \tag{7}$$

where

$$f = 1 - C_pBS/(S^2 + BS + \omega_c{}^2)$$

The filter gain C_p ranges from 0 to 1. For AMB without frequency band rejection, i.e., $C_p = 0$, the complex stiffness as a function of exciting frequency is

$$-F/Y = [K_iG(\Delta C_d + C_v(ab + \omega^2)/(b^2 + \omega^2)) + K_iGC_e\omega_o/(\omega^2 + \omega_o{}^2)]$$
$$+ j\ \omega[K_iGC_v(b - a)/(b^2 + \omega^2) - K_iGC_e/(\omega^2 + \omega_o{}^2)] \tag{8}$$

The real part of equation (8) is the AMB stiffness and the imaginary part is the AMB damping. The second terms of both parts are the main contributors to the AMB "static stiffness" (for small ω). The stiffness and damping of a typical AMB are presented in figure 2. It may appear unusual that the bearing damping can be negative, but as long as no rotor natural vibration mode exists in the frequency range with negative damping, there should be no dynamic problem.

Figure 3 shows the magnitude of the complex stiffnesses for the same AMB with a frequency band rejection. The filter creates a stiffness valley with a depth proportional to C_p. With C_p approaching one, a dynamic force exerted on the rotor at the center frequency can be mostly balanced by the rotor inertia force. Only a small part will be resisted by the AMB and thus transmitted to the bearing stator or ground. In the following section, a potential stability problem of creating such a stiffness valley will be discussed.

AMB STABILITY AT FILTER CENTER FREQUENCY

Figure 4 is a zoomed-in view of the stiffness valley of figure 3. The local complex stiffness decreases and increases sharply but continuously around a center frequency ω_c in a small bandwidth B.

Let

M = rotor mass associated with the AMB

u, v = real and imaginary parts of complex stiffness, respectively, at ω_c before the valley was created

and

$$\sqrt{u/M} > \omega_c$$

which implies a natural frequency exists above the filter center frequency.

Imagine applying a dynamic force to the mass at a frequency ω that is slowly increasing across the valley. There will be (if the valley is deep enough) an exciting frequency, ω_ℓ, associated with a LHS slope stiffness, u_ℓ, such that,

$$\sqrt{u_\ell/M} \simeq \omega_\ell$$

Therefore, ω_ℓ is a resonance frequency. Similarly, there is a RHS slope resonance frequency:

$$\sqrt{u_r/M} \simeq \omega_r$$

These discussions are best illustrated by an example shown in figure 5. Note that these two resonance modes are not due to the filter circuitry alone. They are also related to the mass which the AMB sees. It is of less concern how well the modes are damped. Presumably, if the exciting force frequency, such as the rotor speed, is not drifting away from the filter center frequency, these modes can only be excited by impact type loads. Since the filters are usually implemented with narrow bandwidth, they will not be excited easily as long as they are reasonably damped and no persistant impact load exists. It is a major concern, however, that these modes may not be stable, i.e., associated with positive growth factor or negative damping. This can happen when the gain C_p is made large or approaching one. For example, the LHS slope mode at 59.4 Hz in figure 5 is unstable (growth factor = 120) with $C_p = 1$. It is therefore important in implementing this type of filter to know a threshold stable gain C_p, which is determined in the following analysis.

Let

$$\Delta\omega = \omega_c - \omega$$

and

$$R = (B/2)/\Delta\omega$$

The band-reject factor in equation (7) is

$$f = 1 - C_p(jB\omega)/[(\omega_c^2 - \omega^2) + jB\omega]$$

$$\simeq [1 + (1 - C_p)R^2 - jC_pR]/(1 + R^2) \qquad (9)$$

The complex stiffness around ω_c is approximately

$$-F/Y \simeq (u + jv)\, f = U + jV \qquad (10)$$

where

$$U = u\,[1 - C_pR^2/(1 + R^2)] + v\,C_pR/(1 + R^2) \qquad (11)$$

$$V = v\,[1 - C_pR^2/(1 + R^2)] - u\,C_pR/(1 + R^2) \qquad (12)$$

Both U and V are functions of R, which in turn is a function of the exciting frequency near ω_c. According to equation (12), the RHS mode ($R < 0$) is always more damped than the LHS mode. Note that at the center frequency ($R = \infty$), equations (11) and (12) become

$$U = u\,(1-C_p)$$

and

$$V = v\,(1-C_p)$$

Also note that for effective force isolation, the frequency $\sqrt{[u(1 - C_p)]/M}$ should be one-third of ω_c or less. To determine the threshold gain (C_{po}) for stability, it may not be overly conservative to require

$$V \geq 0$$

which implies by equation (12)

$$C_{po} \leq (1 + R^2)/[(u/v)R + R^2] \tag{13}$$

In the range of 0 to 1, the minimum value of C_{po} occurs at the LHS slope where

$$R = v/u + \sqrt{v^2/u^2 + 1} \tag{14}$$

Incorporating equation (14) into equation (13), the relationship between C_{po} and v/u is plotted in figure 6. For normal AMB applications with $v/u < 1$, the gain value of C_p should be less than 0.83 according to this plot.

STABILITY OF ROTOR-AMB SYSTEM USING FREQUENCY BAND FILTERING

When two or more radial AMBs are supporting a rotor, the mass that each AMB sees is different at different critical modes. The location of the filter center frequency relative to these critical frequencies has a definite influence on the stability problem mentioned above. Since the influence is not straight forward, it would be appropriate to investigate the stability problem in a rotor-AMB dynamic system as follows.

In a conventional rotordynamics approach, the rotor is modeled as sections of circular beams using a finite element method. Concentrated masses and inertias are assigned at the nodes of the beam elements for any attachments to the rotor. Gyroscopic effect is included. For simplicity, circular orbits can be assumed and are adequate for most AMB amplications. For each radial AMB there are two independently controlled axes. For each axis, there is a set of first-order differential equations (FODEs) representing the AMB dynamics. For example, the control scheme of figure 1 can be represented by four FODEs according to equations (4), (5), and (6), which include the frequency band filtering. The rotor-bearing coupling terms exist in equations (2) and (3).

Combining the dynamic equations of the rotor and AMBs, an electromechanical system model can be formulated for eigenvalue evaluation. The formulation procedure is straight forward and will not be presented here. An example eigenvalue analysis for a simple rotor supported by two identical AMBs (fig. 7) is used to demonstrate this system approach. The key AMB control parameters are identical for all four controlled axes (table I). The stiffness and damping of this AMB as functions of frequency have been plotted in figure 2.

Without the filtering, the system has natural modes at 3000 cpm, 10,000 cpm and 35,000 cpm. The rotor-AMB system has been analyzed for the filter centered at 30 Hz and 60 Hz separately. The additional LHS mode, which is less stable than the RHS one, is presented in table II for different values of C_p. The predicted values of C_{po} using equations (13) and (14), as noted on table II, are consistently conservative.

CONCLUSIONS

A frequency band-reject scheme for reducing dynamic force to stator at a selected frequency may create AMB instability problems.

From the generic bearing point of view, this study has shown the following:

1. Depending on the mass supported by the AMB, there can be a natural vibration mode corresponding to the stiffness somewhere on each slope of the stiffness valley. Thus the frequencies of the induced modes are close to the filter center frequency.

2. There is a limit how deep the stiffness valley can be made without causing these modes to be unstable. The limit is related to the local damping-to-stiffness ratio before the valley is created. A conservative limit in terms of the ratio has been established.

From the rotor-AMB system point of view, the AMB mass varies with the rotor critical mode shapes. A rigorous approach to determine the stability is to find the eigenvalues of the electromechanical system.

REFERENCES

1. Weise, D. A.: Active Magnetic Bearings and Their Industrial Applications. 5th Annual Rotating Machinery and Controls Industrial Research Conference, San Antonio, Texas,1985.

2. Habermann, H., and Brunet, M.: The Active Magnetic Bearing Enables Optimum Control of Machine Vibrations. ASME 85-GT-221, 1985.

3. Chen, H. M., and Darlow, M. S.: Design of Active Magnetic Bearings with Velocity Observer. ASME 11th Biennial Conference on Mechanical Vibrations and Noise, Boston, September 1987.

4. Hendrickson, T. A., et al.: Application of Active Magnetic Bearing Technology for Vibration Free Rotating Machinery. Naval Engineers Journal, May 1987, pp. 107-111.

5. Hilburn, J. L., and Johnson, D. E.: Manual of Active Filter Design. McGraw-Hill, 1973.

6. SKF Industries, Inc.: An Introduction to Active Magnetic Bearings. Technology Services Division, King of Prussia, Pennsylvania, June 1981.

TABLE I - RADIAL AMB PARAMETERS

K_i	53.5 N/A
K_m	2.27×10^5 N/m
a	163.3 rad/sec
b	978.8 rad/sec
ω_o	3.14 rad/sec
C_d	5921 volt/m
C_v	5626 volt/m
C_e	31500 volt/m-sec
C_p	0 to 1
ω_c	188.5 rad/sec or 377.0 rad/sec
B	7.54 rad/sec or 15.08 rad/sec

TABLE II - ADDITIONAL LHS MODE

	Speed = 1800 rpm ω_c = 30 Hz; v/u = 0.25; C_{po} = 0.4		Speed = 3600 rpm ω_c = 60 Hz; v/u = 0.46; C_{po} = 0.6	
C_p	Frequency (cpm)	log. decrement	Frequency (cpm)	log. decrement
0.0	1800	0.126	3600	0.126
0.4	1798	0.045	3597	0.064
0.5	1798	0.025	3597	0.049
0.6	1797	0.006 *	3596	0.034
0.8	1796	-0.034 *	3595	0.003 *
1.0	1794	-0.072 *	3593	-0.027 *

* marginal or unstable modes

AN ACTIVE MAGNETIC BEARING CONTROL SCHEME WITH FREQUENCY BAND-REJECT FILTERING

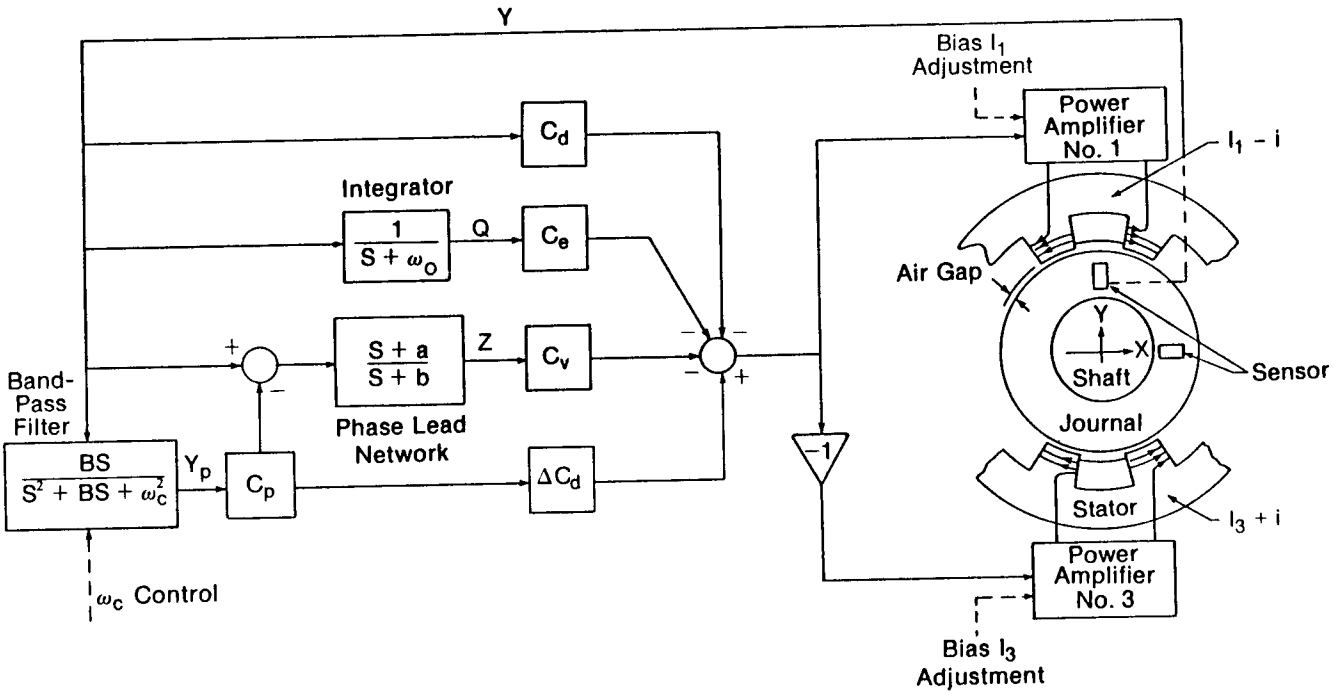

Figure 1

STIFFNESS AND DAMPING OF A TYPICAL ACTIVE MAGNETIC BEARING

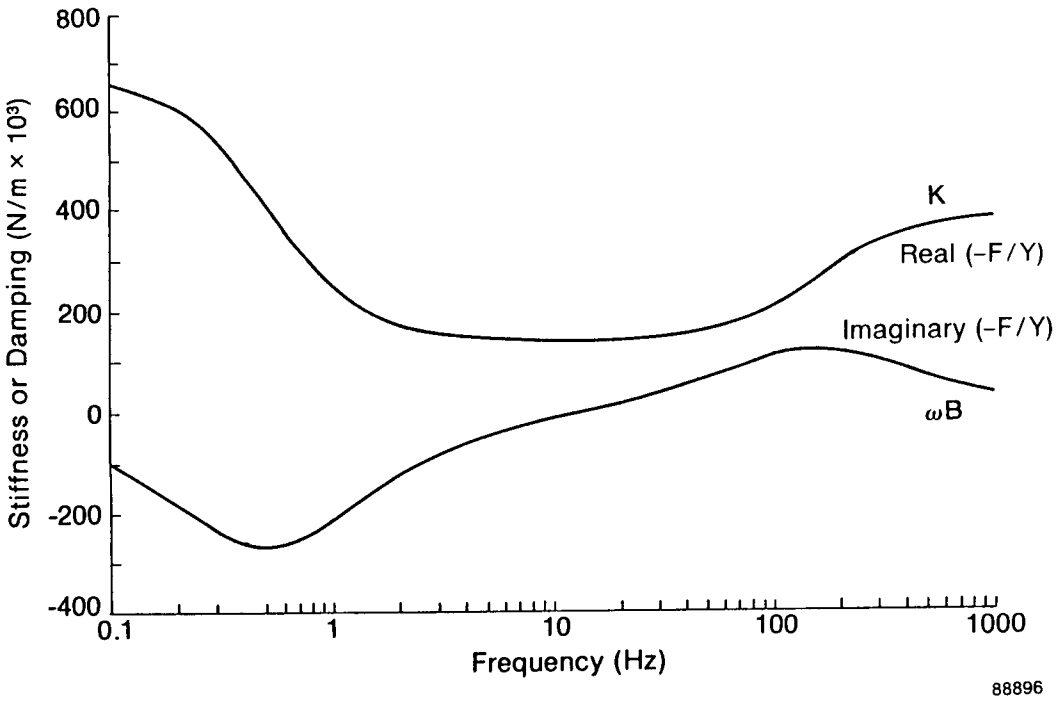

Figure 2

COMPLEX STIFFNESS OF A TYPICAL ACTIVE MAGNETIC BEARING WITH BAND-REJECT FILTERING

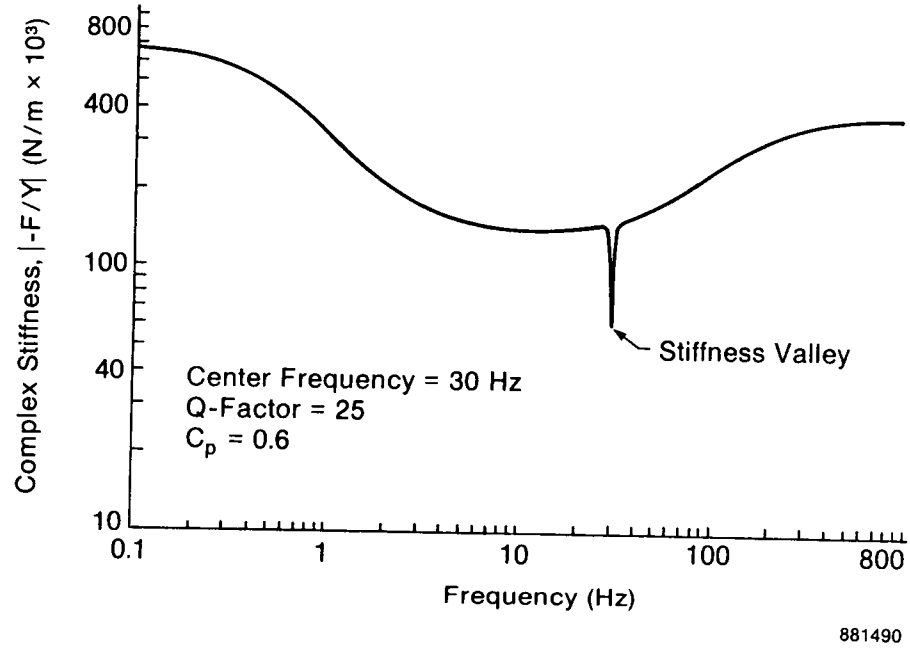

Figure 3

ZOOMED-IN VIEW OF A STIFFNESS VALLEY

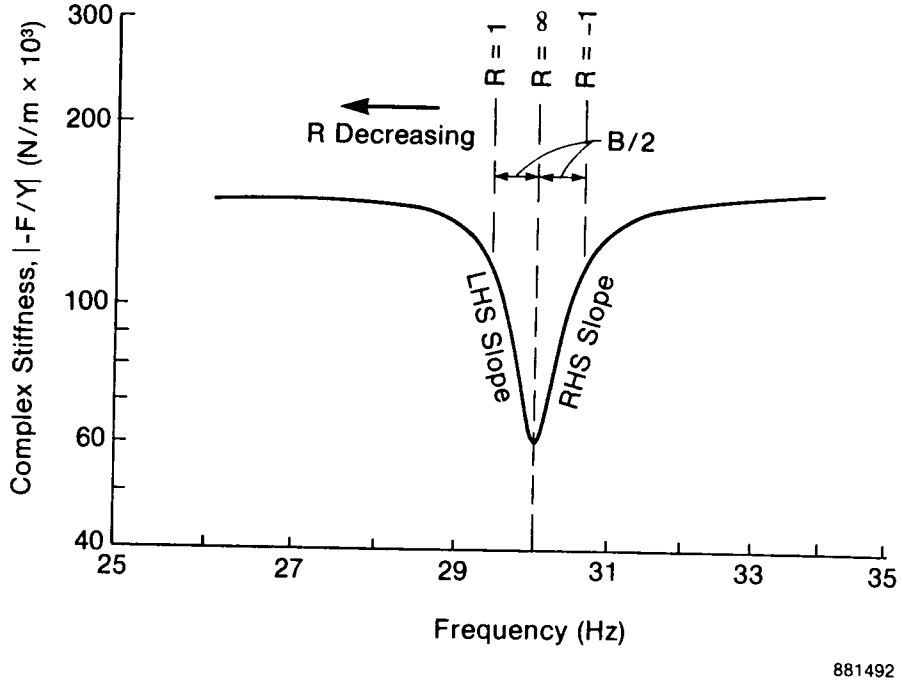

Figure 4

NATURAL FREQUENCY VS. EXCITING FREQUENCY

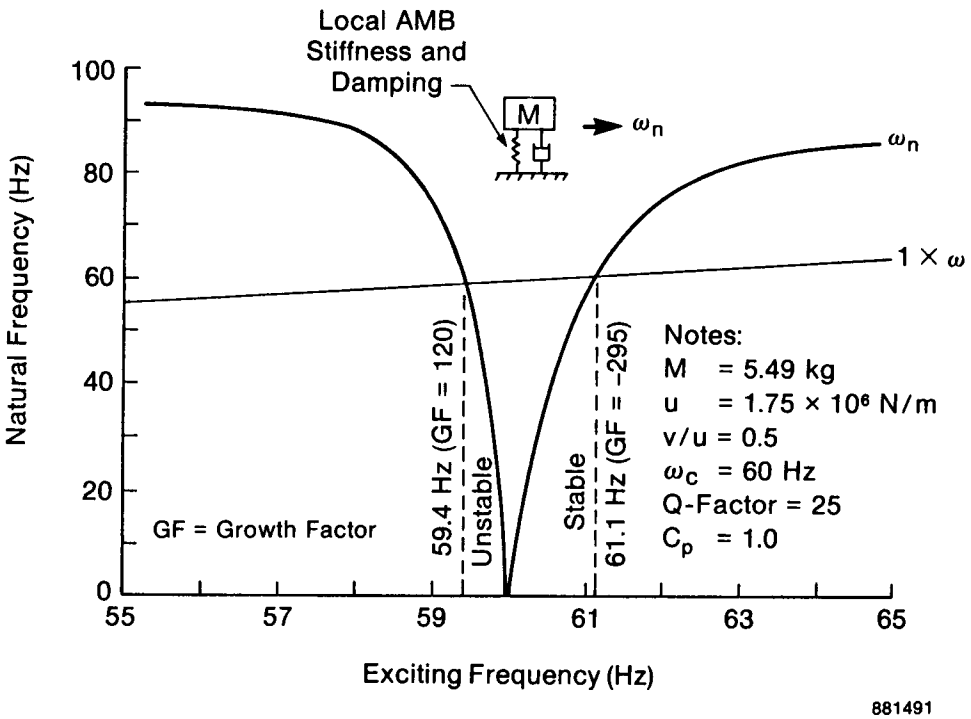

Figure 5

C_{po} VS v/u

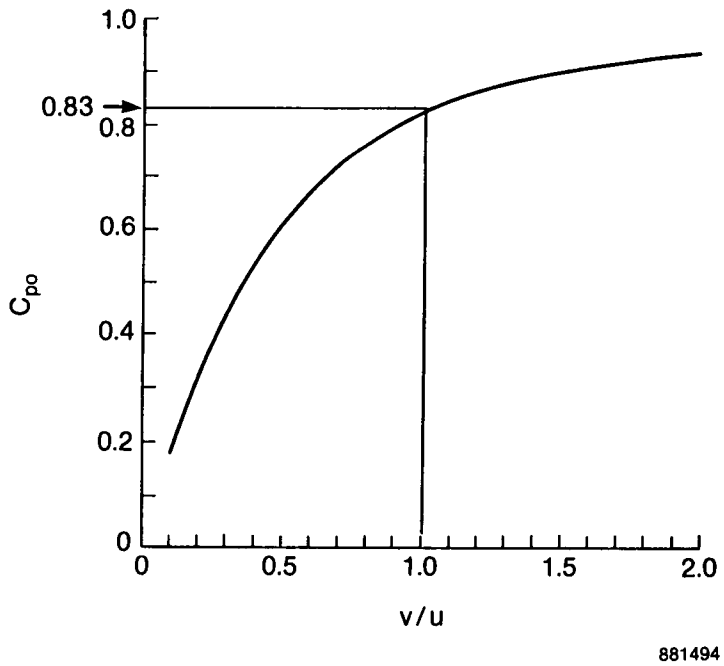

Figure 6

ROTOR MODEL

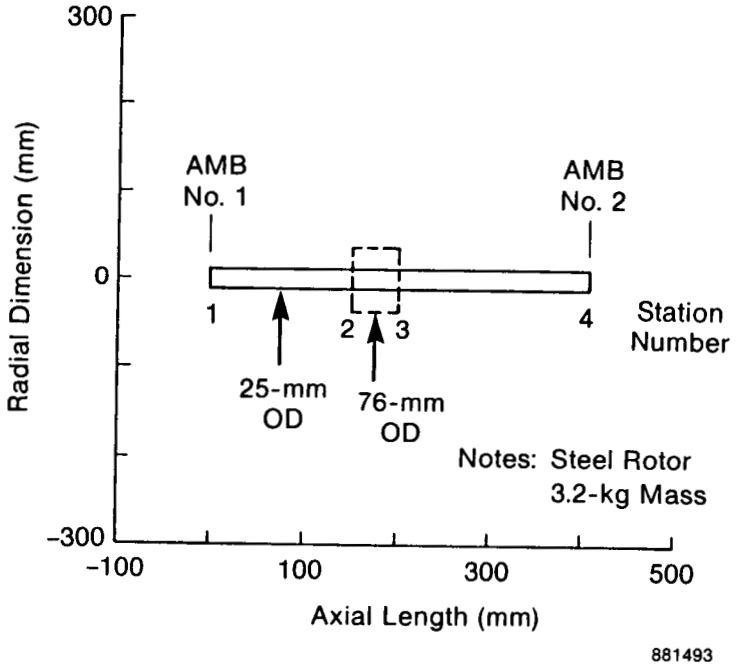

Figure 7